



Contents lists available at ScienceDirect

## Metabolic Engineering

journal homepage: [www.elsevier.com/locate/ymben](http://www.elsevier.com/locate/ymben)

## *Geobacter sulfurreducens* strain engineered for increased rates of respiration

Mounir Izallalen<sup>a,\*</sup>, Radhakrishnan Mahadevan<sup>b</sup>, Anthony Burgard<sup>c</sup>, Bradley Postier<sup>a,1</sup>,  
Raymond Didonato Jr.<sup>a</sup>, Jun Sun<sup>c</sup>, Christopher H. Schilling<sup>c</sup>, Derek R. Lovley<sup>a</sup>

<sup>a</sup> Department of Microbiology, 203 Morrill Science IV-N, University of Massachusetts, Amherst, MA 01003, USA

<sup>b</sup> Department of Chemical Engineering and Applied Chemistry, University of Toronto, Ontario, Canada M5S3E5

<sup>c</sup> Genomatica Inc., 5405 Morehouse Dr., Suite 210, San Diego, CA 92121, USA

## ARTICLE INFO

## Article history:

Received 12 May 2008

Received in revised form

18 June 2008

Accepted 25 June 2008

Available online 27 June 2008

## Keywords:

Geobacter

Genome-based *in silico* modeling

Strain optimization

## ABSTRACT

*Geobacter* species are among the most effective microorganisms known for the bioremediation of radioactive and toxic metals in contaminated subsurface environments and for converting organic compounds to electricity in microbial fuel cells. However, faster rates of electron transfer could aid in optimizing these processes. Therefore, the Optknock strain design methodology was applied in an iterative manner to the constraint-based, *in silico* model of *Geobacter sulfurreducens* to identify gene deletions predicted to increase respiration rates. The common factor in the Optknock predictions was that each resulted in a predicted increase in the cellular ATP demand, either by creating ATP-consuming futile cycles or decreasing the availability of reducing equivalents and inorganic phosphate for ATP biosynthesis. The *in silico* model predicted that increasing the ATP demand would result in higher fluxes of acetate through the TCA cycle and higher rates of NADPH oxidation coupled with decreases in flux in reactions that funnel acetate toward biosynthetic pathways. A strain of *G. sulfurreducens* was constructed in which the hydrolytic, F<sub>1</sub> portion of the membrane-bound F<sub>0</sub>F<sub>1</sub> (H<sup>+</sup>)-ATP synthase complex was expressed when IPTG was added to the medium. Induction of the ATP drain decreased the ATP content of the cell by more than half. The cells with the ATP drain had higher rates of respiration, slower growth rates, and a lower cell yield. Genome-wide analysis of gene transcript levels indicated that when the higher rate of respiration was induced transcript levels were higher for genes involved in energy metabolism, especially in those encoding TCA cycle enzymes, subunits of the NADH dehydrogenase, and proteins involved in electron acceptor reduction. This was accompanied by lower transcript levels for genes encoding proteins involved in amino acid biosynthesis, cell growth, and motility. Several changes in gene expression that involve processes not included in the *in silico* model were also detected, including increased expression of a number of redox-active proteins, such as c-type cytochromes and a putative multicopper outer-surface protein. The results demonstrate that it is possible to genetically engineer increased respiration rates in *G. sulfurreducens* in accordance with predictions from *in silico* metabolic modeling. To our knowledge, this is the first report of metabolic engineering to increase the respiratory rate of a microorganism.

© 2008 Elsevier Inc. All rights reserved.

### 1. Introduction

*Geobacter* species have a number of unique properties that could conceivably be enhanced for practical applications. For example, *Geobacter* species are highly effective in completely oxidizing organic compounds to carbon dioxide under anaerobic conditions with electron transfer to metals (Lovley et al., 1993, 1991, 1987; Lovley and Phillips, 1988) or electrodes (Bond et al., 2002; Bond and Lovley, 2003; Lovley, 2006a).

Oxidation of organic contaminants coupled to the reduction of naturally occurring Fe(III) oxides (Lovley et al., 1989) can play an important role in the natural attenuation of contaminated groundwater and this process can be artificially stimulated with the addition of Fe(III) chelators (Lovley et al., 1994) or electron shuttle compounds (Lovley et al., 1996) to enhance contaminant degradation. *Geobacter* species can precipitate toxic and/or radioactive metals such as uranium by using these metals as a terminal electron acceptor, reducing the oxidized, soluble form of the metals to insoluble reduced forms (Anderson et al., 2003; Lovley et al., 1991; Ortiz-Bernad et al., 2004). Oxidation of organic compounds coupled to electron transfer to electrodes offers the possibility of converting a range of organic waste materials and renewable biomass to electricity (Lovley, 2006a, b).

\* Corresponding author. Fax: +1 413 545 1578.

E-mail address: [imounir@microbio.umass.edu](mailto:imounir@microbio.umass.edu) (M. Izallalen).

<sup>1</sup> Present address: Department of Biology, University of Washington in St. Louis, St. Louis, MO 63130.

Fast rates of extracellular electron transfer are desired for these applications of *Geobacter* species. However, it is likely that most *Geobacter* species have evolved in sedimentary environments in which there has been little selective pressure for rapid metabolism of electron donors. Constraint-based modeling (CBM) offers the possibility to predict metabolic network fluxes from annotated genomes (Price et al., 2004). Rather than attempting to predict exactly how the cell will behave, the constraint-based approach narrows the range of possible phenotypes that a cellular system can display through successive imposition of governing physico-chemical constraints such as stoichiometry, thermodynamics, and enzyme capacity (Palsson, 2000; Price et al., 2003; Schilling and Palsson, 1998). In recent applications of CBM, the outcome of adaptive evolution and gene expression changes in regulatory mutants of *Escherichia coli* were successfully predicted (Covert et al., 2004; Ibarra et al., 2002). Expanding on the CBM approach, the Optknock framework suggests gene deletions strategies leading to the overproduction of specific chemical products (Burgard and Maranas, 2003). This is achieved by a bilevel optimization that ensures the coupling of growth to the biosynthesis of the product of interest. The computational procedure is designed to identify not just straightforward but also non-intuitive knockout strategies by simultaneously considering the entire metabolic network (Pharkya et al., 2003; Reed et al., 2003).

In order to increase the rate of extracellular electron transport in *Geobacter sulfurreducens* we coupled the recently completed genome-based *in silico* metabolic model of *G. sulfurreducens* (Mahadevan et al., 2006) to the computational framework Optknock to devise metabolic engineering strategies. Here we report that a variety of gene deletions are predicted to result in increased respiration in *G. sulfurreducens*. Each of these possible mutations increases ATP consumption in the cell via futile cycles or other means. Insertion of an ATP drain in *G. sulfurreducens* resulted in physiological changes in accordance with model predictions.

## 2. Material and methods

### 2.1. Strains and media

*G. sulfurreducens* (Table 1) was routinely cultivated following strict anaerobic methods (N<sub>2</sub>/CO<sub>2</sub> [80:20, vol:vol]) in NBAF medium as described previously (Coppi et al., 2001), with 15 mM acetate as the electron donor and 40 mM fumarate as the electron acceptor. Where indicated, fumarate was replaced with 55 mM Fe(III) citrate. *E. coli* strain One Shot<sup>®</sup> DH5 $\alpha$ <sup>™</sup> (Invitrogen, Carlsbad, CA) and *E. coli* S17-1<sub>pir</sub> (Table 1) were routinely cultivated on Luria-Bertani (LB) broth and plates. Antibiotics were purchased from Sigma (St. Louis, MO) and used to a final concentration of 50  $\mu$ g/ml kanamycin and 100  $\mu$ g/ml ampicillin

for *E. coli* and at 200  $\mu$ g/ml of kanamycin for *G. sulfurreducens* recombinant strains. Concentrations of isopropyl  $\beta$ -D-thiogalactopyranoside (IPTG) varied according to the experimental conditions as noted.

### 2.2. Optknock simulations

The Optknock strain design methodology (Burgard et al., 2003) was applied within an iterative framework to identify multiple sets of knockouts leading the coupling of electron generation to cell growth in *G. sulfurreducens*. The genome-scale metabolic model of *G. sulfurreducens* (Mahadevan et al., 2006) served as the backbone of this analysis. The iterative procedure entailed solving the Optknock problem with the incorporation of an additional constraint referred to as an integer cut at each iteration. Integer cut constraints effectively prevent the solution procedure from choosing the exact same set of knockouts identified in any previous iteration. Multiple knockout strategies were identified assuming growth on an acetate substrate with fumarate or Fe(III) serving as the electron acceptors. The final result for each carbon substrate/electron acceptor pair was a ranked list, in terms of maximum electron yield (i.e., maximum reduction of the available electron acceptor) at optimal growth, of distinct deletion strategies that differ from one another by at least one knockout.

### 2.3. Recombinant DNA techniques

Chromosomal DNA of *G. sulfurreducens* was extracted from fumarate-grown cells using the MasterPure<sup>™</sup> DNA purification kit (Epicentre Biotechnologies, Madison, WI). The *atpA*, *atpG*, and *atpD* genes from *G. sulfurreducens* were PCR amplified using the primers F-*atpAGD* 5'-GACCCAGTTGACCAGGATTCAGG-3' and R-*atpAGD* 5'-CGCTGAATTCACCCAGCGCAG-3' purchased from Sigma-Genosys (The Woodlands, TX) and by the Accutag<sup>™</sup> LA DNA polymerase (Sigma, St. Louis, MO). The PCR conditions were as follows: an initial denaturation step of 6 min at 96 °C followed by 30 cycles consisting of 1 min at 94 °C for denaturation, 30 s at 65 °C for annealing and an extension of 4 min at 68 °C. Amplified DNA was purified using the Qiaquick gel extraction kit (Qiagen, Valencia, CA) and cloned in the pCR2.1 vector using the TOPO cloning kit (Invitrogen). The positive clone was digested with *EcoRI* to release the *atpAGD* module. The *EcoRI* digested fragment was ligated into the pCD341 shuttle vector (Dehio et al., 1998). The resulting plasmid pAGD was electroporated into *G. sulfurreducens* following in-house standard molecular procedures (Coppi et al., 2001).

### 2.4. Analytical techniques

Organic acids were determined using an HP series 1100 high-pressure liquid chromatograph (Hewlett-Packard, Palo Alto, CA)

**Table 1**  
Strains and plasmids used in this work

Strain or plasmid	Description <sup>a</sup>	Reference or source
<i>Geobacter sulfurreducens</i> DL1	Wild-type strain	(Caccavo et al., 1994), ATCC 51573
<i>Escherichia coli</i> One shot <sup>®</sup> DH5 $\alpha$ <sup>™</sup>	F <sup>-</sup> <i>mcrA</i> $\Delta$ ( <i>mrr</i> - <i>hsdRMS</i> - <i>mcrBC</i> ) $\phi$ 80 <i>lacZ</i> $\Delta$ M15 $\Delta$ <i>lacX74</i> <i>recA1</i> <i>araD139</i> $\Delta$ ( <i>araleu</i> ) <i>galJ</i> <i>galK</i> <i>rpsL</i> <i>endA1</i>	Invitrogen Corp.
<i>E. coli</i> S17-1 <sub>pir</sub>	( $\lambda$ <sub>pir</sub> ) <i>thi</i> <i>pro</i> <i>RecA</i> <i>hsdR</i> RP4-2- <i>tet</i> ::Mu <i>aphA</i> ::Tn7	(Miller and Mekalanos, 1988)
pCD342	Wide-host range cloning vector, IPTG inducible, Kan <sup>R</sup>	(Dehio et al., 1998)
PAGD	pCD342 derivative containing <i>atpAGD</i> genes from <i>G. sulfurreducens</i>	This work
DL1-pCD	<i>G. sulfurreducens</i> containing native pCD342 shuttle plasmid, Kan <sup>R</sup>	This work
DL1-pAGD	<i>G. sulfurreducens</i> containing the pAGD vector, Kan <sup>R</sup>	This work

<sup>a</sup> Kan<sup>R</sup> denotes resistance to kanamycin.

equipped with a UV detector (210 nm). Products were separated using a Bio-Rad HPX-87H column with 4 mM H<sub>2</sub>SO<sub>4</sub> as the mobile phase. Fe(III) reduction was measured by the ferrozine assay as described previously (Lovley and Phillips, 1986). The respiration rate  $q_{\text{electron}}$  was calculated from the reduced form of the electron acceptor as described previously (Esteve-Nunez et al., 2005). ATP was measured with the Bac Titer-Glo™ microbial cell viability assay (Promega, Madison, WI) against a standard curve made with ATP (Promega). The ATP was quantified by measuring relative fluorescence units on a TD-20/20 luminometer (Turner-Design, Sunnyvale, CA). Total proteins were extracted with the B-PER nonanionic detergent and were quantified with BCA reagent (Pierce, Rockford, IL) using bovine serum albumin (BSA) as a standard. Cell densities of Fe(III)-grown cultures were measured by epifluorescence microscopy using acridine orange staining (Lovley and Phillips, 1988).

### 2.5. RNA extraction

Mid-log phase 100 ml cultures of DL1-pAGD ( $O \times D_{600} = 0.2$ ) and DL1-pCD ( $O \times D_{600} = 0.3$ ) growing on NBAF+2 mM IPTG were centrifuged at 4000 rpm, 4 °C for 10 min. Total RNA was extracted from the bacterial pellet using the RNeasy midi kit (Qiagen, Valencia, CA). Purified RNA was DNA-free™ DNase (Ambion®, Austin, TX) treated to remove contaminating DNA. Aliquots from treated samples were subjected to PCR amplification with specific *G. sulfurreducens* primers to validate the absence of genomic DNA. The extracted RNA was labeled using the ASAP® RNA Labeling kit (PerkinElmers, Boston, MA). Briefly, 10 µg RNA from DL1-pAGD+2 mM IPTG (experimental sample) and DL1-pCD+2 mM IPTG (control sample) were labeled with cyanin3 (cy3) and cyanin5 (cy5), respectively. Unbound cy3 and cy5 were removed by purification of the labeling reaction through Microcon spin columns (Millipore, Bedford, MA). Purified RNA was chemically fragmented using the fragmentation reagent product from Ambion®. RNA fragments were ethanol precipitated and washed three times with 70% ethanol and resuspended in a 20 µl final volume of RNase-free water.

### 2.6. Array design

The microarrays were designed using the genomic sequence of *G. sulfurreducens* (accession number AE17180.1). The microarrays consisted of 12,000 electrochemically synthesized oligonucleotides (3.3 probes per gene) spotted on Customarray™ 12K

(Combimatrix, Mukilteo, WA) as previously described (Postier et al., 2008).

### 2.7. Hybridization, washing and scanning

CustomArray™ 12K slides (Combimatrix, Mukilteo, WA) were washed, prehybridized and hybridized with labeled and fragmented RNA following manufacturer's recommendation. The arrays were scanned in a Genepix 4000B scanner (Molecular Device Inc., Sunnyvale, CA) and images were analyzed using both GenePix and Acuity 4.0 software (Molecular Device Inc.). The total intensity of each outlined spot was exported into the R package for statistical analysis.

### 2.8. Statistical analysis

Background signal was calculated from negative control spotted onto the slides. These controls are universal in all the microarrays and sometimes cross-hybridize with tested samples. The background value was determined using 30% of the lowest intensity controls, and set to be equal to the mean+2 standard deviation. Only probes with signal intensity higher than the background were further analyzed. We applied Lowess global normalization on the ratio  $M$  [ $M = \log_2(\text{cy3}/\text{cy5})$ ]. Normalized data was subjected to LIMMA mixed model analysis. LIMMA calculates a moderated  $t$  statistic for each probe corresponding to the ratio of the estimated mean logged intensity ratio and the empirical Bayes estimate of its standard error. The  $p$  value of each probe is corrected for multiple comparisons to control false discovery rates (Benjamini and Hochberg, 1995). Probes were ranked by the adjusted  $p$ -values and were called differentially expressed if the adjusted  $p$ -values were <0.05 (or <0.001 for the stringent case). For each gene the multiple oligonucleotides probes were analyzed separately and genes were called differentially expressed if at least half of their probes were called differentially expressed.

## 3. Results

### 3.1. Optknock analysis

Analysis of *G. sulfurreducens* metabolism with the previously described constraint-based model (Mahadevan et al., 2006) and the Optknock algorithm identified a number of deletions in genes

**Table 2**

Optknock proposed reaction deletions: the reactions are grouped by the physiological impact of their deletion

Reactions	Equations
<i>Increase in ATP demand</i>	
Malate dehydrogenase	Mal-L+NAD ↔ H+NADH+oaa
Pyruvate phosphate dikinase	ATP+pyruvate+phosphate ↔ AMP+phosphoenolpyruvate+diphosphate
ammonium transporter	NH <sub>4</sub> [e] ↔ NH <sub>4</sub> [c]
Glycine hydroxymethyltransferase	5,10-methylenetetrahydrofolate+glycine+H <sub>2</sub> O ↔ tetrahydrofolate+L-serine
<i>Decrease in reducing equivalents availability</i>	
Phosphoglycerate dehydrogenase	3-phospho-D-glycerate+NAD(+) ↔ 3-phosphonoxy pyruvate+NADH
Glutamate synthase (ferredoxin)	2 L-glutamate+2 oxidized ferredoxin ↔ L-glutamine+2-oxoglutarate+2 reduced ferredoxin
Glutamate dehydrogenase (NADP)	L-glutamate+H <sub>2</sub> O+NADP(+) ↔ 2-oxoglutarate+NH <sub>3</sub> +NADPH
Tetradecanoyl-[acyl-carrier protein] malonyl :CoA C-acyltransferase	Acyl-[acyl-carrier-protein]+NADP(+) ↔ trans-2,3-dehydroacyl-[acyl-carrier-protein]+NADPH
3-oxoacyl-[acyl-carrier-protein]:NADP oxido-reductase	(3R)-3-hydroxyacyl-[acyl-carrier-protein]+NADP(+) ↔ 3-oxoacyl-[acyl-carrier-protein]+NADPH
<i>Decrease in inorganic phosphate (pi) availability</i>	
Phosphoserine phosphatase	L(or D)-O-phosphoserine+H <sub>2</sub> O ↔ L(or D)-serine+phosphate
inorganic diphosphatase (one proton translocation)	Diphosphate+H <sub>2</sub> O ↔ 2 phosphate
phosphate transport in/out via proton symporter	H[e]+pi[e] ↔ H[c]+pi[c]

[e] :extracytoplasmic, [c] cytoplasmic.

involved in the central metabolism or amino acid and fatty acid metabolism that would increase the rate of respiration (Table 2). All the Optknock predictions targeted gene deletions resulting in an increased cellular ATP demand. Such strategies comprised the creation of ATP-consuming futile cycles as well as mechanisms lowering the availability of reducing equivalents and inorganic phosphate for ATP biosynthesis. For example, the greatest increases in electron flux were predicted to be associated with the deletion of the genes for malate dehydrogenase or ammonium uptake. With acetate as the electron donor, the TCA cycle is the main source of reducing equivalents for *G. sulfurreducens* (Galushko and Schink, 2000). The model indicated that, in the absence of malate dehydrogenase, oxaloacetate can be formed via the combined reactions of the malic enzyme and pyruvate carboxylase. However, this pathway consumes an ATP. Deletion of the ammonium transporter requires that *G. sulfurreducens* fix atmospheric nitrogen to satisfy its nitrogen requirements (Coppi et al., 2001). Nitrogen fixation is an energetically demanding process (Simpson and Burris, 1984) that requires the hydrolysis of 16 ATP for each fixed nitrogen molecule. Elimination of dehydrogenases of various biosynthetic pathways involved in forming NADH or NADPH decreases the amount of reducing equivalents that would have otherwise reached the electron transport chain, thus reducing the amount of ATP generated from respiration.

### 3.2. In silico analysis of inserting an ATP drain

In order to broadly examine the impact of an imposed ATP drain on the metabolism of *G. sulfurreducens* the *in silico* model of *G. sulfurreducens* was modified to include additional consumption of ATP that was simulated by increasing the values of the ATP maintenance ( $ATP_M$ ). The  $ATP_M$  corresponds to the rate of ATP consumption associated with non-biosynthetic functions (Tempest and Neijssel, 1984). The model predicted a linear relationship between an increase in  $ATP_M$  costs, and a decrease in the growth rate (Fig. 1). Decreasing growth rate correlated with an increase in the respiration rate (Fig. 1). This was true whether the simulations were run with fumarate or Fe(III) as the electron acceptor.

The introduction of an ATP drain that corresponded to the highest non-lethal  $ATP_M$  value resulted in predicted increases in fluxes in reactions catalyzed by several TCA cycle enzymes such as fumarate reductase, fumarase, malate dehydrogenase, citrate synthase, aconitase, isocitrate dehydrogenase, and 2-oxoglutarate synthase (Table 3). Increases in flux were also predicted for the acetate CoA-transferase reaction, which connects the acetate activation to the TCA cycle (Galushko and Schink, 2000). The flux of the NADPH dehydrogenase reaction involved in the transfer of electrons into the respiratory chain was also predicted to increase. In contrast, there were predicted significant decreases in the fluxes for the reactions catalyzed by acetate kinase and phosphoacetyl transferase, reactions that direct the acetate away from the TCA cycle and towards assimilation in the gluconeogenic pathway in which pyruvate oxido-reductase and pyruvate kinase are involved (Segura et al., 2008). Decreased fluxes through several biosynthetic pathways were also predicted in response to increased ATP consumption (Table 3).

### 3.3. Physiological impact on addition of an ATP drain to *G. sulfurreducens*

In order to experimentally evaluate the impact of an ATP drain on the physiology of *G. sulfurreducens*, a strain was constructed which contained a plasmid with the *atpAGD* genes under the control of the inducible *pta*lacUV5 promoter. These genes encode

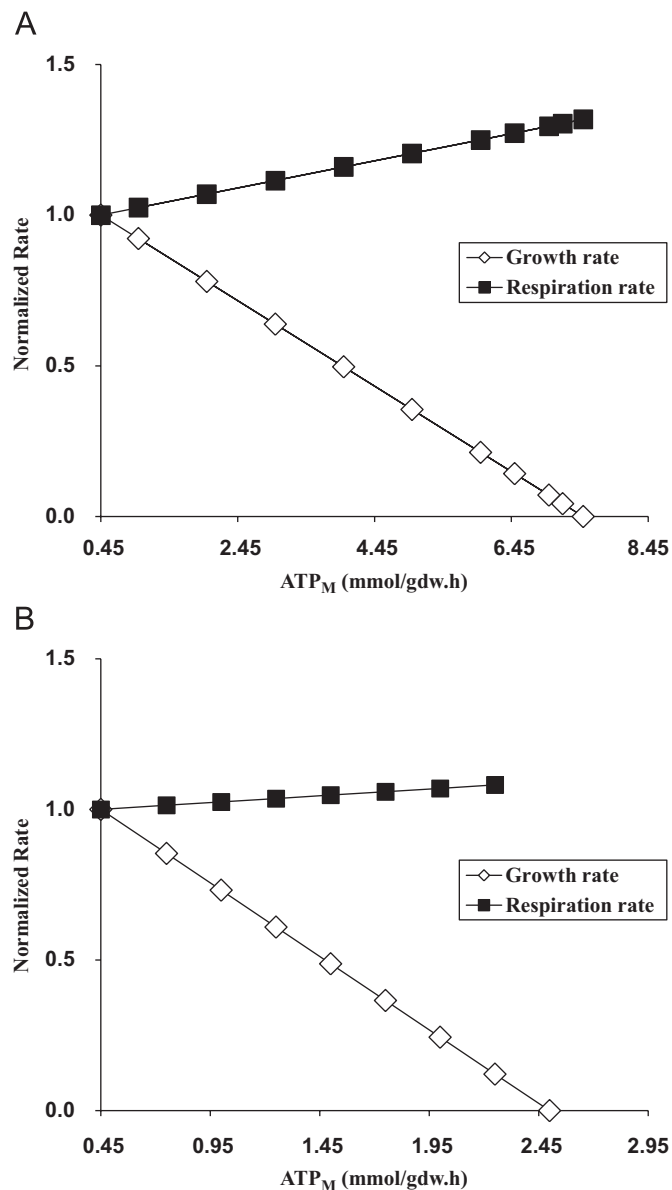


Fig. 1. Impact on predicted respiration and biomass production rates in cultures growing with fumarate (A) or Fe(III) (B) when an additional ATP consumption was added to the *G. sulfurreducens* *in silico* model by increasing the ATP maintenance values.

the hydrolytic,  $F_1$  portion of the membrane-bound  $F_0F_1$  ( $H^+$ )-ATP synthase complex. Under full induction of the *atpAGD* genes, the ATP content of the cells was 0.09 nmol ATP/mg cell protein, which is substantially lower than the 0.21 nmol of ATP/mg cell protein in the strain bearing the control vector. The control strain grew as well as wild-type cells, even when IPTG was added. However, when the *atpAGD* genes were on the plasmid, the addition of IPTG resulted in a higher rate of respiration, a slower growth rate, and a lower final cell yield (Fig. 2 and Table 4). Cells with the ATP drain expressed had growth rates that were only 37% and 42% of the control strain, for cells grown with fumarate or Fe(III) as the electron acceptor, respectively (Table 4).

Although the biomass yield  $Y_{acetate}$  decreased by 64% in the presence of the ATP drain, the specific consumption rate of acetate was the same as in the absence of the ATP drain. Thus, the decrease in growth in the presence of the ATP drain was not the result of decreased availability of acetate.

**Table 3**  
Comparison of predicted flux distribution in central metabolism reactions during normal and high ATP demand growth

Equation	Normal growth	Growth with an ATP drain	Enzyme name
accoa+pi $\leftrightarrow$ actp+coa	0.863	0.061	Phosphotransacetylase
ac+atp $\leftrightarrow$ actp+adp	0.863	0.061	Acetate kinase
coa+fdxo-4:2+pyr $\leftrightarrow$ accoa+co2+fdxr-4:2+h	0.508	0.036	Pyruvate oxido-reductase
atp+pi+pyr $\rightarrow$ amp+h+pep+ppi	0.275	0.019	Pyruvate phosphate dikinase
3pg $\leftrightarrow$ 2pg	0.244	0.017	Phosphoglycerate mutase
2pg $\leftrightarrow$ h2o+pep	0.244	0.017	Enolase
g3p+nad+pi $\leftrightarrow$ 13dpg+h+nadh	0.184	0.013	Glyceraldehyde 3P dehydrogenase
13dpg+adp $\leftrightarrow$ 3pg+atp	0.184	0.013	Phosphoglycerate kinase
atp+hco3+pyr $\rightarrow$ adp+h+oaa+pi	0.115	0.008	Pyruvate carboxylase
fdp+h2o $\rightarrow$ f6p+pi	0.078	0.006	Fructose biphosphatase
fdp $\leftrightarrow$ dhap+g3p	0.078	0.006	Fructose biphosphate aldolase
dhap $\leftrightarrow$ g3p	0.078	0.006	Triose phosphate isomerase
g6p $\leftrightarrow$ f6p	0.053	0.004	Glucose 6P isomerase
cit $\leftrightarrow$ icit	4.206	4.944	Aconitase
icit+nadp $\leftrightarrow$ akg+co2+nadph	4.206	4.944	Isocitrate dehydrogenase (NADP)
accoa+h2o+oaa $\rightarrow$ cit+coa+h	4.206	4.944	Citrate synthase
fum+h2o $\leftrightarrow$ mal-L	4.192	4.943	Fumarase
mal-L+nad $\leftrightarrow$ h+nadh+oaa	4.192	4.943	Malate dehydrogenase
akg+coa+fdxo-4:2 $\rightarrow$ co2+fdxr-4:2+h+succoa	4.164	4.941	2-oxoglutarate synthase
ac+succoa $\rightarrow$ accoa+succ	4.150	4.940	Acetate CoA transferase
akg+fdxr-4:2+gln-L+(2)h $\leftrightarrow$ fdxo-4:2+(2) glu-L	3.725	4.910	Glutamate synthase
fdxr-4:2+h+nadp $\leftrightarrow$ fdxo-4:2+nadph	7.381	9.814	Ferredoxine (NADP) reductase
fum+mql7 $\leftrightarrow$ mqn7+succ	11.02	14.718	Fumarate reductase
(3) h[c]+mqn7[c]+nadph[c] $\rightarrow$ (2)h[e]+mql7[c]+nadp[c]	11.006	14.717	NADPH dehydrogenase
fum[e]+succ[c] $\leftrightarrow$ fum[c]+succ[e]	15.180	19.658	Succinate:fumarate exchanger

Fluxes are expressed as mmol/gdw h.

**Abbreviations:** accoa: acetyl CoA, actp: acetyl phosphate, coa: coenzyme A, fdxo-4:2: ferredoxine oxidized form 4:2, pyr: pyruvate, fdxr-4:2: ferredoxine reduced form 4:2, pep: phosphoenolpyruvate, pi: phosphate, ppi: diphosphate, 3pg: 3-phospho-D-glycerate, D-glycerate-2-phosphate, g3p: glyceraldehyde 3-phosphate, 13dpg: 3-phospho-D-glycerol phosphate, 3pg: 3-phospho-D-glycerate, hco3: bicarbonate, oaa: oxaloacetate, fdp: D-fructose 1,6-biphosphate, f6p: D-fructose 6-phosphate, dhap: dihydroxyacetone phosphate, g6p: D-glucose 6-phosphate, cit: citrate, icit: isocitrate, akg: 2-oxoglutarate, fum: fumarate, mal-L: L-malate, succoa: succinyl CoA, mqn7: menaquinone, gln-L: L-glutamine, glu-L: L-glutamate.

### 3.4. Microarray analysis

In order to determine how the higher rates of respiration in the presence of the ATP drain impacted gene expression, the gene transcript levels in cells induced to express *atpAGD* was compared to transcript levels in the control strain, also exposed to IPTG during growth with fumarate as the electron acceptor. In general, genes which had higher transcript levels in the presence of the ATP drain encode enzymes involved in energy metabolism and respiration (Table 5) whereas genes with lower transcript levels encode enzymes involved in biosynthesis and flagellar motility (Table 6). As expected, there was a substantial increase in transcripts encoding the *atpAGD* module which was induced with IPTG (Table 5). There was also an increase in the expression of the ATP synthase  $\epsilon$  subunit (GSU0114) corresponding to *atpC*. This protein is part of the stalk that connects the soluble  $F_0$  portion to the  $F_1$  membrane domain of the  $F_0F_1$ -ATP synthase and plays an important role in the switching of the motor action of the ATP synthase (Tsunoda et al., 2001; Wilkens et al., 1995). This gene was not included in the cloned and inducible ATPase encoding module.

Numerous genes encoding TCA cycle enzymes were up-regulated when the additional ATP-consuming reaction was induced with IPTG. Transcript levels for *frdA* and *frdB*, which encode the two subunits of the bifunctional fumarate reductase and succinate dehydrogenase (Butler et al., 2006), significantly increased under IPTG-inducing conditions. There was also an increase in transcripts for *dcuB* during growth with the ATP drain. This gene encodes for the fumarate/succinate antiporter that is required for transport of fumarate into the cell to be utilized as an electron acceptor (Butler et al., 2006). The increase in fumarate reductase and fumarate transporter transcripts would theoretically provide the cell with an improved capacity to reduce

fumarate. The transcript levels for two other TCA enzymes, the eukaryotic like citrate synthase (Bond et al., 2005) and the aconitate hydratase (*acnB*) were also up-regulated. However, transcript levels for some genes encoding TCA cycle enzymes, such as the genes for malate dehydrogenase (*mdh*), isocitrate dehydrogenase (*icd*), 2-oxoglutarate synthase (*oorABCD*) and the fumarase (*fumB*) did not change during growth with the additional ATP-consuming reaction.

There was also a significant increase in transcripts of genes involved in cellular energy generation (Table 5). There were higher transcript levels for several genes of the *nuo* cluster, which encode the large-membrane-associated NADH dehydrogenase that transfers reducing equivalents generated in the TCA cycle to the menaquinone pool. Increases in gene expression were also observed in the three subunits of the respiratory hydrogenase complex *hybLAB* that has been shown to be essential for *G. sulfurreducens* to oxidize  $H_2$  (Coppi et al., 2004). The three putative acetate transporters and the acetyl-CoA-transferase (*ato*) maintained similar expression levels in the presence of the ATP drain, but transcript levels for the gene for the acetate kinase (*ack*) involved in the activation of acetate to acetyl phosphate declined (Table 6). This differential expression would provide more enzymes for the dissimilation of acetate in the TCA cycle than assimilation via gluconeogenesis (Segura et al., 2008).

Several genes involved in the biosynthesis of the bacterial peptidoglycan and encoding for the MUR proteins (*murA*, *murC*, and *murE*) were down-regulated during growth with high ATP demand (Table 6). Additionally, multiple genes responsible for flagella biosynthesis were down-regulated. Two genes *flgC* and *flgG* that compose the proximal and distal rod proteins located in the basal body (Saijo-Hamano et al., 2004) had lower transcript levels as did *fliR* and *fliQ* that are both involved in flagellar biosynthesis protein (Ohnishi et al., 1997), *fliN*, the flagellar motor

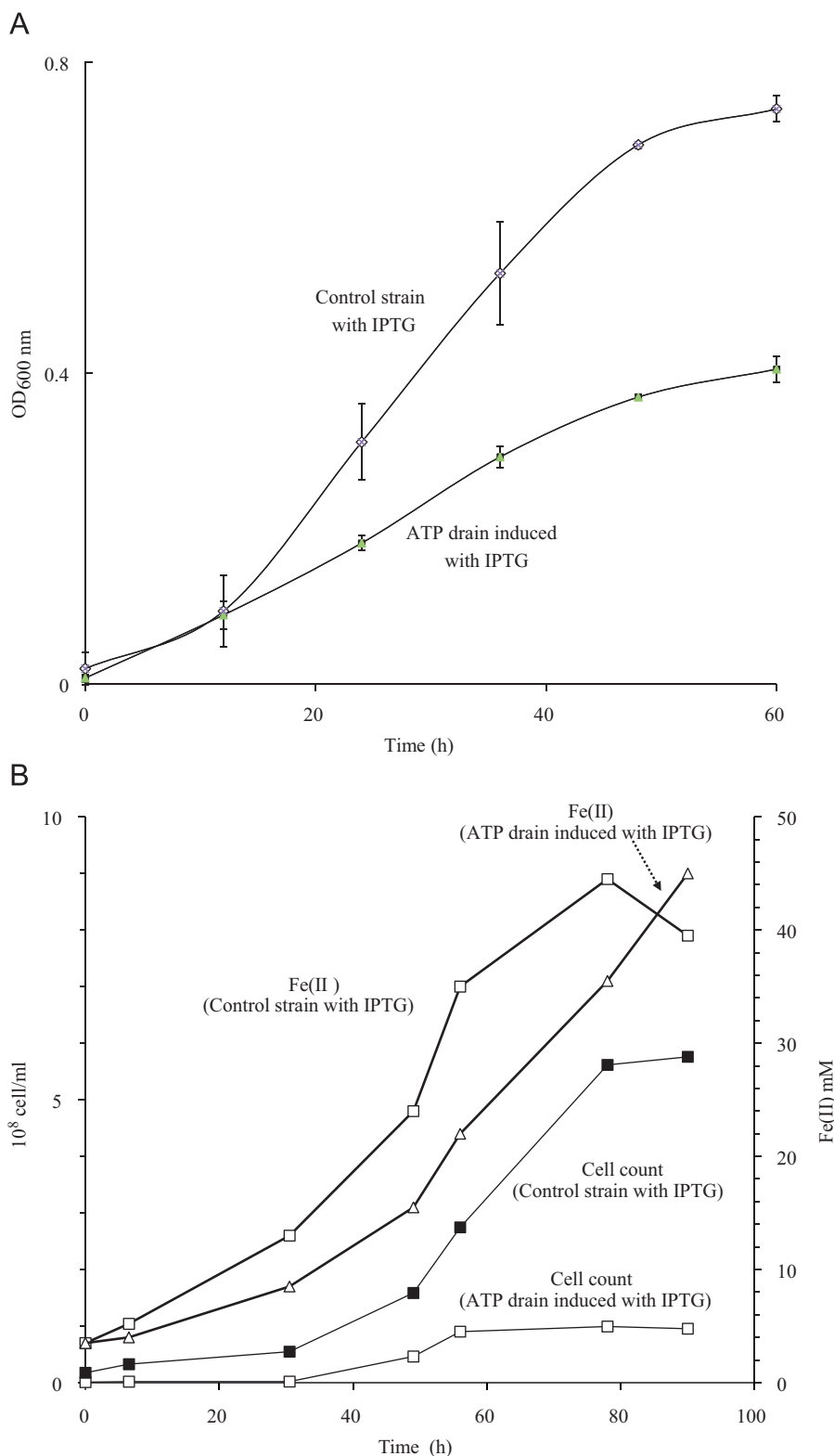


**Fig. 2.** Effect of the induction of cloned *atpAGD* in *G. sulfurreducens* DL1-pAGD during growth with fumarate (A) or Fe(III) citrate (B) as terminal electron acceptors in comparison to the control strain containing the empty plasmid DL1-pCD.

switch protein (Paul et al., 2006), and *fliI*, a membrane-bound ATPase that provides energy for the export of proteins by the secretory apparatus (Stephens et al., 1997).

Several amino acid biosynthesis genes also had lower transcript levels in the presence of the ATP drain (Table 6). These included (amino acid biosynthesis affected in parentheses): *trpE*

and *trpC* (tryptophane); *aroB* (tryptophane, phenylalanine, and tyrosine); *hisD* (histidine); *argC* (arginine); *proC* (proline); *argH* (arginine); and *cysE* (serine).

A number of genes which are not included in the *in silico* model also had significant changes in transcript levels. For example, genes for a number of redox-active proteins had increased

**Table 4**

Metabolic parameters measured during growth in the presence of the ATP drain induced in the recombinant strain containing the *atpAGD* module and in the control strain containing the plasmid without the *atpAGD* module

Metabolic parameters	Control	ATP drain
$\mu$ (fumarate) <sup>a</sup>	0.08	0.05
$\mu$ (FeIII) <sup>a</sup>	0.07	0.04
$q_{\text{acetate}}$ (mmol/gdw h) <sup>b</sup>	5.67	5.58
$Y_{\text{acetate}}$ <sup>c</sup> (mg dw/mmol acetate)	14	9
Fumarate respiration $q_{\text{electron}}$ (mmol electrons/gdw h)	16.55	19.17
Fe(III) respiration $q_{\text{electron}}$ (mmol electrons/cell h) <sup>d</sup>	$1.21 \times 10^{-9}$	$1.71 \times 10^{-9}$

<sup>a</sup>  $\mu$ : growth rate with fumarate or Fe(III) as terminal electron acceptors (TEA).

<sup>b</sup>  $q_{\text{acetate}}$ : acetate consumption rate during growth with fumarate as the terminal electron acceptor.

<sup>c</sup>  $Y_{\text{acetate}}$ : cell yield during growth with fumarate as the terminal electron acceptor.

<sup>d</sup> Expressed as per cell rather than per mg dry weight because the low number of cells precluded accurate weight determination.

transcript levels (Table 5). These included *omcB*, which encodes a polyheme outer-membrane *c*-type cytochrome required for optimal Fe(III) reduction (Leang et al., 2003) and *ppcB* and *ppcC*, which encode periplasmic *c*-type cytochromes (L. Didonato, unpublished data). There was also an increase in the expression of *oxpG*, which encodes a predicted component of the type II secretory pathway associated with the translocation of the multicopper protein OmpB (Mehta et al., 2006). Transcripts for the OmpB gene were also higher in the presence of the ATP drain.

#### 4. Discussion

The results demonstrate that, as predicted with genome-scale *in silico* metabolic modeling, the addition of an ATP drain increased respiration rates in *G. sulfurreducens*, with a concurrent decrease in cell growth and biomass yield. To our knowledge, this is the first report of metabolic engineering to increase the respiratory rate of a microorganism. As detailed below, increasing

**Table 5**

Genes with significantly higher transcript levels in fumarate-grown *G. sulfurreducens* containing the IPTG-induced *atpAGD* genes compared to the control strain

Gene symbol	Locus name	Fold change	Cellular roles	Common name
<i>atpA</i>	GSU0111	2.54	Energy metabolism	ATP synthase F1, $\alpha$ subunit
<i>atpG</i>	GSU0112	2.35	Energy metabolism	ATP synthase F1, $\gamma$ subunit
<i>atpD</i>	GSU0113	2.32	Energy metabolism	ATP synthase F1, $\beta$ subunit
<i>atpC</i>	GSU0114	1.71	Energy metabolism	ATP synthase F1, $\epsilon$ subunit
<i>fba</i>	GSU1245	1.57	Energy metabolism	Fructose-bisphosphate aldolase
<i>frdA</i>	GSU1177	1.38	Energy metabolism	Fumarate reductase, flavoprotein subunit
<i>frdB</i>	GSU1176	1.32	Energy metabolism	Fumarate reductase
<i>acnB</i>	GSU1660	1.33	Energy metabolism	Aconitate hydratase 2
<i>dcuB</i>	GSU2751	1.29	Transport	C4-dicarboxylate transporter, anaerobic
<i>pgi</i>	GSU1311	1.28	Energy metabolism	Glucose-6-phosphate isomerase
<i>cs</i>	GSU1106	1.28	Energy metabolism	Citrate synthase
<i>nuoL-2</i>	GSU3434	1.36	Energy metabolism	NADH dehydrogenase I, I subunit
<i>nuoL-1</i>	GSU0349	1.35	Energy metabolism	NADH dehydrogenase I, L subunit
<i>nuoK</i>	GSU0348	1.30	Energy metabolism	NADH dehydrogenase I, K subunit
<i>hybB</i>	GSU0784	1.51	Energy metabolism	Nickel-dependent hydrogenase, membrane protein
<i>hybA</i>	GSU0783	1.47	Energy metabolism	Nickel-dependent hydrogenase, iron-sulfur cluster
<i>hybL</i>	GSU0785	1.34	Energy metabolism	Nickel-dependent hydrogenase, large subunit
<i>ccdA</i>	GSU1322	1.71	Energy metabolism	Cytochrome <i>c</i> biogenesis protein
<i>omcB</i>	GSU2737	1.38	Energy metabolism	Polyheme membrane-associated cytochrome <i>c</i>
<i>ppcB</i>	GSU0364	1.37	Energy metabolism	Cytochrome <i>c3</i>
<i>oxpG</i>	GSU1776	1.59	TypeII secretion system	Pilin domain protein
<i>ompB</i>	GSU1394	1.35	Unknown function	Multicopper protein

**Table 6**

Genes with significantly lower transcript levels in fumarate-grown *G. sulfurreducens* containing the IPTG-induced *atpAGD* genes compared to the control strain

Gene symbol	Locus name	Fold change	Cellular roles	Common name
<i>ack</i>	GSU3448	0.72	Central intermediary metabolism	Acetate kinase
<i>hisD</i>	GSU3100	0.61	Amino acid biosynthesis	Histidinol dehydrogenase
<i>trpE</i>	GSU2383	0.73	Amino acid biosynthesis	Anthranilate synthase component I
<i>gltA</i>	GSU3057	0.74	Amino acid biosynthesis	Glutamate synthase (NADPH), homotetrameric
<i>aroB</i>	GSU2025	0.75	Amino acid biosynthesis	3-dehydroquinate synthase
<i>argC</i>	GSU2874	0.75	Amino acid biosynthesis	<i>N</i> -acetyl- $\gamma$ -glutamyl-phosphate reductase
<i>trpC</i>	GSU2380	0.76	Amino acid biosynthesis	Indole-3-glycerol phosphate synthase
<i>proC</i>	GSU2541	0.79	Amino acid biosynthesis	Pyrroline-5-carboxylate reductase
<i>argH</i>	GSU0156	0.70	Amino acid biosynthesis	Argininosuccinate lyase
<i>murE</i>	GSU3074	0.76	Cell envelope	UDP- <i>N</i> -acetylmuramoylalanyl-D-glutamyl-2,6-diaminopimelate ligase
<i>murC</i>	GSU3068	0.78	Cell envelope	UDP- <i>N</i> -acetylmuramate-alanine ligase
<i>murA</i>	GSU3102	0.71	Cell envelope	UDP- <i>N</i> -acetylglucosamine 1-carboxyvinyltransferase
<i>flgC</i>	GSU0408	0.64	Cellular processes	Flagellar basal-body rod protein
<i>flgG</i>	GSU3052	0.64	Cellular processes	
<i>flil</i>	GSU0413	0.75	Energy metabolism	Flagellum-specific ATP synthase
<i>flitR</i>	GSU0425	0.68	Cellular processes	Flagellar biosynthesis protein
<i>flitN</i>	GSU0422	0.52	Cellular processes	Flagellar motor switch protein
<i>flitQ</i>	GSU0424	0.64	Cellular processes	Flagellar biosynthetic protein

the rate of respiration in *Geobacter* species is of special interest because extracellular electron transfer has a number of practical applications.

#### 4.1. Physiological response to ATP drain—comparison with studies in *E. coli*

The impact on metabolism of introducing an ATP drain in *G. sulfurreducens* differs substantially from what was previously observed in *E. coli*. Depleting ATP in *E. coli* growing on glucose, by overexpressing the F1 subunit of the membrane-bound F<sub>0</sub>F<sub>1</sub> (H<sup>+</sup>)-ATP synthase in order to lower the [ATP]/[ADP] ratio (Koebmman et al., 2002) or deleting the F<sub>1</sub>-ATPase to abolish oxidative phosphorylation (Noda et al., 2006) increased glycolytic flux during glucose oxidation, but the carbon flow was directed toward acetate secretion rather than complete oxidation via the TCA cycle with associated increased respiration rates. In *E. coli* the expression of genes for TCA cycle enzymes in the presence of an ATP drain was less than in wild-type cells. This is an adaptive response because the high rates of glycolysis in the ATP-depleted cells generate excess NADH, and limiting the TCA cycle reduces further NADH generation.

In contrast, because *G. sulfurreducens* grows on acetate, and can only generate ATP via respiration, it needs to increase flux through the TCA cycle and the rate of respiration in order to produce more ATP in response to an ATP drain. The *in silico* metabolic model predicted this increase in TCA cycle. The ATP drain triggered also an unexpected regulatory response that resulted in a higher expression of genes encoding TCA cycle enzymes and the subunits for the NADH dehydrogenase required to transfer the NADH generated from the TCA cycle to the electron transport chain.

The increased demand for respiratory activity in response to an ATP drain was evidenced by an increase in transcript levels for the genes encoding fumarate reductase subunits. Increases in transcripts for one of these genes, *frdA*, were previously shown to be directly related to increases in the rate of fumarate respiration (Chin et al., 2004). This adaptation to high respiration rate is also achieved by increasing the fumarate transporter expression, increasing the supply of the terminal electron acceptor. Increases in transcripts of genes, such as *omcB* and *ompB*, that are associated with Fe(III) reduction are also probably the result of a general response to a low-energy physiological status (Esteve-Nunez et al., 2005).

The *in silico* model predicted that the metabolic perturbation caused by the increase in ATP consumption would reduce the fluxes towards biomass formation. The decrease in *ack* transcript levels interestingly reflects this prediction, because acetate assimilation into biomass starts by the Ack-mediated phosphorylation of acetate to Acetyl-P (Galushko and Schink, 2000). Therefore, a decrease in this pathway will decrease the availability of carbon to be funneled towards gluconeogenesis and other anabolic branches. This is another instance where the prediction of the *in silico* model and the measured gene expression have a similar trend. The decrease in transcripts of genes involved in amino acid biosynthesis as a response to low ATP levels indicates another possible cellular control of ATP-consuming reactions. The down-regulation of amino acid biosynthesis genes and *ack* would contribute to a decrease in biomass formation and growth rate. The need to decrease ATP consumption might also account for the lower transcript abundance for several flagellar genes because the synthesis of the flagellum and its operation for bacterial motility are energetically expensive (Armitage, 1999). The apparent up-regulation of the  $\epsilon$  subunit of the F<sub>1</sub>F<sub>0</sub>-ATP synthase, shown previously to be involved in coupling the catalytic site activities and proton translocation, as well as the inhibition of ATP hydrolysis (Feniouk et al., 2007), may be indicative of an

additional response in *G. sulfurreducens* to prevent ATP waste during the futile ATP consumption.

In this work, we encountered several instances where the trends in the metabolic model predicted fluxes correlated with measured transcript levels. However, making an inference of metabolic fluxes from transcriptional profiles is precarious because of the absence of correlation between gene expression and enzyme activity (ter Kuile and Westerhoff, 2001), the difficulty of predicting the directionality in reversible reactions, or the lack of knowledge of post-transcriptional modifications (Yang et al., 2002). Conversely, data derived from transcriptional analysis provides additional information that has been used to improve flux prediction in metabolic modeling (Akeson et al., 2004; Covert and Palsson, 2002).

#### 4.2. Potential applications

The incentive for these studies was that faster extracellular electron transfer may have applications for bioremediation and the production of electricity in microbial fuel cells. For example, the *in situ* bioremediation of uranium-contaminated groundwater relies upon the ability of *Geobacter* species to reduce soluble U(VI) to insoluble U(IV) (Anderson et al., 2003; Finneran et al., 2002; Lovley et al., 1991). For this application, it is preferable to reduce metals as rapidly as possible without accumulating excess biomass that might fill pore spaces and impact on groundwater flow. In microbial fuel cells the goal is to have high rates of oxidation of organic fuels with electron transfer to the fuel cell anode. The more fuel oxidized and the less fuel incorporated into biomass the more efficient the microbial fuel cell. Inducing the ATP drain in the strain described here does not result in more current in microbial fuel cells than that produced by wild-type cells (data not shown), demonstrating that there are other microbiological or electrochemical impediments to higher current production.

However, these studies demonstrate the power of *in silico* modeling to aid in developing strategies for altering the metabolism and potential function of microorganisms with practical applications. Other model-inspired modifications of *G. sulfurreducens* that may have applications for bioremediation and current production are underway.

#### Acknowledgments

This material is based upon work supported by the National Science Foundation under Grant No. NSF-2-2006 1001 and by the Office of Science (BER), U.S. Department of Energy, Cooperative Agreement No. DE-FC02-02ER63446.

#### References

- Akeson, M., Forster, J., Nielsen, J., 2004. Integration of gene expression data into genome-scale metabolic models. *Metab. Eng.* 6 (4), 285–293.
- Anderson, R.T., Vrionis, H.A., Ortiz-Bernad, I., Resch, C.T., Long, P.E., Dayvault, R., Karp, K., Marutzky, S., Metzler, D.R., Peacock, A., White, D.C., Lowe, M., Lovley, D.R., 2003. Stimulating the *in situ* activity of *Geobacter* species to remove uranium from the groundwater of a uranium-contaminated aquifer. *Appl. Environ. Microbiol.* 69 (10), 5884–5891.
- Armitage, J.P., 1999. Bacterial tactic responses. *Adv. Microb. Physiol.* 41, 229–289.
- Benjamini, Y., Hochberg, Y., 1995. Controlling the false discovery rate—a practical and powerful approach to multiple testing. *J. R. Stat. Soc. B* 57 (1), 289–300.
- Bond, D.R., Lovley, D.R., 2003. Electricity production by *Geobacter sulfurreducens* attached to electrodes. *Appl. Environ. Microbiol.* 69 (3), 1548–1555.
- Bond, D.R., Holmes, D.E., Tender, L.M., Lovley, D.R., 2002. Electrode-reducing microorganisms that harvest energy from marine sediments. *Science* 295 (5554), 483–485.
- Bond, D.R., Mester, T., Nesbo, C.L., Izquierdo-Lopez, A.V., Collart, F.L., Lovley, D.R., 2005. Characterization of citrate synthase from *Geobacter sulfurreducens* and

- throughout the Geobacteraceae. Appl. Environ. Microbiol. 71 (7), 3858–3865.
- Burgard, A.P., Maranas, C.D., 2003. Optimization-based framework for inferring and testing hypothesized metabolic objective functions. Biotechnol. Bioeng. 82 (6), 670–677.
- Burgard, A.P., Pharkya, P., Maranas, C.D., 2003. OptKnock: a bilevel programming framework for identifying gene knockout strategies for microbial strain optimization. Biotechnol. Bioeng. 84 (6), 647–657.
- Butler, J.E., Glaven, R.H., Esteve-Nunez, A., Nunez, C., Shelobolina, E.S., Bond, D.R., Lovley, D.R., 2006. Genetic characterization of a single bifunctional enzyme for fumarate reduction and succinate oxidation in *Geobacter sulfurreducens* and engineering of fumarate reduction in *Geobacter metallireducens*. J. Bacteriol. 188 (2), 450–455.
- Caccavo Jr., F., Lonergan, D.J., Lovley, D.R., Davis, M., Stolz, J.F., McNerney, M.J., 1994. *Geobacter sulfurreducens* sp. nov., a hydrogen- and acetate-oxidizing dissimilatory metal-reducing microorganism. Appl. Environ. Microbiol. 60 (10), 3752–3759.
- Chin, K.J., Esteve-Nunez, A., Leang, C., Lovley, D.R., 2004. Direct correlation between rates of anaerobic respiration and levels of mRNA for key respiratory genes in *Geobacter sulfurreducens*. Appl. Environ. Microbiol. 70 (9), 5183–5189.
- Coppi, M.V., Leang, C., Sandler, S.J., Lovley, D.R., 2001. Development of a genetic system for *Geobacter sulfurreducens*. Appl. Environ. Microbiol. 67 (7), 3180–3187.
- Coppi, M.V., O'Neil, R.A., Lovley, D.R., 2004. Identification of an uptake hydrogenase required for hydrogen-dependent reduction of Fe(III) and other electron acceptors by *Geobacter sulfurreducens*. J. Bacteriol. 186 (10), 3022–3028.
- Covert, M.W., Palsson, B.O., 2002. Transcriptional regulation in constraints-based metabolic models of *Escherichia coli*. J. Biol. Chem. 277 (31), 28058–28064.
- Covert, M.W., Knight, E.M., Reed, J.L., Herrgard, M.J., Palsson, B.O., 2004. Integrating high-throughput and computational data elucidates bacterial networks. Nature 429 (6987), 92–96.
- Dehio, M., Knorre, A., Lanz, C., Dehio, C., 1998. Construction of versatile high-level expression vectors for *Bartonella henselae* and the use of green fluorescent protein as a new expression marker. Gene 215 (2), 223–229.
- Esteve-Nunez, A., Rothermich, M., Sharma, M., Lovley, D., 2005. Growth of *Geobacter sulfurreducens* under nutrient-limiting conditions in continuous culture. Environ. Microbiol. 7 (5), 641–648.
- Feniouk, B.A., Suzuki, T., Yoshida, M., 2007. Regulatory interplay between proton motive force, ADP, phosphate, and subunit epsilon in bacterial ATP synthase. J. Biol. Chem. 282 (1), 764–772.
- Finneran, K.T., Housewright, M.E., Lovley, D.R., 2002. Multiple influences of nitrate on uranium solubility during bioremediation of uranium-contaminated subsurface sediments. Environ. Microbiol. 4 (9), 510–516.
- Galushko, A.S., Schink, B., 2000. Oxidation of acetate through reactions of the citric acid cycle by *Geobacter sulfurreducens* in pure culture and in syntrophic coculture. Arch. Microbiol. 174 (5), 314–321.
- Ibarra, R.U., Edwards, J.S., Palsson, B.O., 2002. *Escherichia coli* K-12 undergoes adaptive evolution to achieve *in silico* predicted optimal growth. Nature 420 (6912), 186–189.
- Koebmann, B.J., Westerhoff, H.V., Snoep, J.L., Nilsson, D., Jensen, P.R., 2002. The glycolytic flux in *Escherichia coli* is controlled by the demand for ATP. J. Bacteriol. 184 (14), 3909–3916.
- Leang, C., Coppi, M.V., Lovley, D.R., 2003. OmcB, a c-type polyheme cytochrome, involved in Fe(III) reduction in *Geobacter sulfurreducens*. J. Bacteriol. 185 (7), 2096–2103.
- Lovley, D.R., 2006a. Bug juice: harvesting electricity with microorganisms. Nat. Rev. Microbiol. 4 (7), 497–508.
- Lovley, D.R., 2006b. Microbial fuel cells: novel microbial physiologies and engineering approaches. Curr. Opin. Biotechnol. 17 (3), 327–332.
- Lovley, D.R., Phillips, E.J., 1986. Organic matter mineralization with reduction of ferric iron in anaerobic sediments. Appl. Environ. Microbiol. 51 (4), 683–689.
- Lovley, D.R., Phillips, E.J., 1988. Novel mode of microbial energy metabolism: organic carbon oxidation coupled to dissimilatory reduction of iron or manganese. Appl. Environ. Microbiol. 54 (6), 1472–1480.
- Lovley, D.R., Stolz, J.F., Nord, G.L., Phillips, E.J.P., 1987. Anaerobic production of magnetite by a dissimilatory iron-reducing microorganism. Nature 330 (6145), 252–254.
- Lovley, D.R., Baedeker, M.J., Lonergan, D.J., Cozzarelli, I.M., Phillips, E.J.P., Siegel, D.I., 1989. Oxidation of aromatic contaminants coupled to microbial iron reduction. Nature 339 (6222), 297–300.
- Lovley, D.R., Phillips, E.J.P., Gorby, Y.A., Landa, E.R., 1991. Microbial reduction of uranium. Nature 350, 413–416.
- Lovley, D.R., Giovannoni, S.J., White, D.C., Champine, J.E., Phillips, E.J., Gorby, Y.A., Goodwin, S., 1993. *Geobacter metallireducens* gen. nov. sp. nov., a microorganism capable of coupling the complete oxidation of organic compounds to the reduction of iron and other metals. Arch. Microbiol. 159 (4), 336–344.
- Lovley, D.R., Woodward, J.C., Chapelle, F.H., 1994. Stimulated anoxic biodegradation of aromatic hydrocarbons using Fe(III) ligands. Nature 370 (6485), 128–131.
- Lovley, D.R., Coates, J.D., Blunt-Harris, E.L., Phillips, E.J.P., Woodward, J.C., 1996. Humic substances as electron acceptors for microbial respiration. Nature 382 (6590), 445–448.
- Mahadevan, R., Bond, D.R., Butler, J.E., Esteve-Nunez, A., Coppi, M.V., Palsson, B.O., Schilling, C.H., Lovley, D.R., 2006. Characterization of metabolism in the Fe(III)-reducing organism *Geobacter sulfurreducens* by constraint-based modeling. Appl. Environ. Microbiol. 72 (2), 1558–1568.
- Mehta, T., Childers, S.E., Glaven, R., Lovley, D.R., Mester, T., 2006. A putative multicopper protein secreted by an atypical type II secretion system involved in the reduction of insoluble electron acceptors in *Geobacter sulfurreducens*. Microbiology 152 (Pt. 8), 2257–2564.
- Miller, V.L., Mekalanos, J.J., 1988. A novel suicide vector and its use in construction of insertion mutations: osmoregulation of outer membrane proteins and virulence determinants in *Vibrio cholerae* requires toxR. J. Bacteriol. 170 (6), 2575–2583.
- Noda, S., Takezawa, Y., Mizutani, T., Asakura, T., Nishiumi, E., Onoe, K., Wada, M., Tomita, F., Matsushita, K., Yokota, A., 2006. Alterations of cellular physiology in *Escherichia coli* in response to oxidative phosphorylation impaired by defective F1-ATPase. J. Bacteriol. 188 (19), 6869–6876.
- Ohnishi, K., Fan, F., Schoenhals, G.J., Kihara, M., Macnab, R.M., 1997. The FliQ, FliP, FliQ, and FliR proteins of *Salmonella typhimurium*: putative components for flagellar assembly. J. Bacteriol. 179 (19), 6092–6099.
- Ortiz-Bernad, I., Anderson, R.T., Vrionis, H.A., Lovley, D.R., 2004. Vanadium respiration by *Geobacter metallireducens*: novel strategy for *in situ* removal of vanadium from groundwater. Appl. Environ. Microbiol. 70 (5), 3091–3095.
- Palsson, B., 2000. The challenges of *in silico* biology. Nat. Biotechnol. 18 (11), 1147–1150.
- Paul, K., Harmon, J.G., Blair, D.F., 2006. Mutational analysis of the flagellar rotor protein FliN: identification of surfaces important for flagellar assembly and switching. J. Bacteriol. 188 (14), 5240–5248.
- Pharkya, P., Burgard, A.P., Maranas, C.D., 2003. Exploring the overproduction of amino acids using the bilevel optimization framework OptKnock. Biotechnol. Bioeng. 84 (7), 887–899.
- Postier, B., Didonato Jr., R., Nevin, K.P., Liu, A., Frank, B., Lovley, D., Methe, B.A., 2008. Benefits of *in-situ* synthesized microarrays for analysis of gene expression in understudied microorganisms. J. Microbiol. Methods 74 (1), 26–32.
- Price, N.D., Papin, J.A., Schilling, C.H., Palsson, B.O., 2003. Genome-scale microbial *in silico* models: the constraints-based approach. Trends Biotechnol. 21 (4), 162–169.
- Price, N.D., Reed, J.L., Palsson, B.O., 2004. Genome-scale models of microbial cells: evaluating the consequences of constraints. Nat. Rev. Microbiol. 2 (11), 886–897.
- Reed, J.L., Vo, T.D., Schilling, C.H., Palsson, B.O., 2003. An expanded genome-scale model of *Escherichia coli* K-12 (iJR904 GSM/GPR). Genome Biol. 4 (9), R54.
- Saijo-Hamano, Y., Uchida, N., Namba, K., Oosawa, K., 2004. *In vitro* characterization of FlgB, FlgC, FlgF, FlgG, and FliE, flagellar basal body proteins of *Salmonella*. J. Mol. Biol. 339 (2), 423–435.
- Schilling, C.H., Palsson, B.O., 1998. The underlying pathway structure of biochemical reaction networks. Proc. Natl. Acad. Sci. USA 95 (8), 4193–4198.
- Segura, D., Mahadevan, R., Juarez, K., Lovley, D.R., 2008. Computational and experimental analysis of redundancy in the central metabolism of *Geobacter sulfurreducens*. PLoS Comput. Biol. 4 (2), e36.
- Simpson, F.B., Burris, R.H., 1984. A nitrogen pressure of 50 atmospheres does not prevent evolution of hydrogen by nitrogenase. Science 224 (4653), 1095–1097.
- Stephens, C., Mohr, C., Boyd, C., Maddock, J., Gober, J., Shapiro, L., 1997. Identification of the flil and flj components of the *Caulobacter* flagellar type III protein secretion system. J. Bacteriol. 179 (17), 5355–5365.
- Tempest, D.W., Neijssel, O.M., 1984. The status of YATP and maintenance energy as biologically interpretable phenomena. Annu. Rev. Microbiol. 38, 459–486.
- ter Kuile, B.H., Westerhoff, H.V., 2001. Transcriptome meets metabolome: hierarchical and metabolic regulation of the glycolytic pathway. FEBS Lett. 500 (3), 169–171.
- Tsunoda, S.P., Rodgers, A.J., Aggeler, R., Wilce, M.C., Yoshida, M., Capaldi, R.A., 2001. Large conformational changes of the epsilon subunit in the bacterial F<sub>1</sub>F<sub>0</sub> ATP synthase provide a ratchet action to regulate this rotary motor enzyme. Proc. Natl. Acad. Sci. USA 98 (12), 6560–6564.
- Wilkins, S., Dahlquist, F.W., McIntosh, L.P., Donaldson, L.W., Capaldi, R.A., 1995. Structural features of the epsilon subunit of the *Escherichia coli* ATP synthase determined by NMR spectroscopy. Nat. Struct. Biol. 2 (11), 961–967.
- Yang, C., Hua, Q., Shimizu, K., 2002. Integration of the information from gene expression and metabolic fluxes for the analysis of the regulatory mechanisms in *Synechocystis*. Appl. Microbiol. Biotechnol. 58 (6), 813–822.